

August 1976

LRP 115/76

FINITE ELEMENT APPROXIMATION FOR THE WAVE-PARTICLE
INTERACTION IN WEAKLY TURBULENT PLASMA

K. Appèrt, T.M. Tran, J. Vaclavik

Centre de Recherches en Physique des Plasmas
ECOLE POLYTECHNIQUE FEDERALE DE LAUSANNE

FINITE ELEMENT APPROXIMATION FOR THE WAVE-PARTICLE
INTERACTION IN WEAKLY TURBULENT PLASMA

K. Appert, T.M. Tran, J. Vaclavik

ABSTRACT

A finite element method is presented for the numerical treatment of two-dimensional quasilinear equations. The method is applied to the electron-beam-plasma interaction. Strong influence of the initial fluctuation level on the evolution of the turbulence has been found.

1. INTRODUCTION

15 years after the first pioneering work in plasma turbulence [1] most essential problems still remain unsolved. The reason for this bad situation lies in the nonlinearities inherent to the turbulent phenomena. The interactions in a real physical system are most often so strong as to inhibit a perturbative treatment as is done in the so-called weak turbulence theory (WTT). And since a consistent non-perturbative strong turbulence theory does not yet exist, numerical experiments using particle pushing methods seem to be the only resort.

However, in the past few years it has become clear that the finiteness of computational budgets imposes severe limitations on the physical content in particle simulations. It is for example, unimaginable that microscopic physics modelled by standard particle simulation could be build into an MHD transport or laser-fusion code. On the other hand heuristic transport coefficients may be too coarse a picture of the turbulent phenomena. What is felt now is the lack of simple and numerically cheap models able to describe at least the most important nonlinear physics correctly.

Regarded from this point of view, WTT appears in a new light. It appears as an important reservoir of rather simple models. In fact the domain of applicability of certain equations may be larger than their theoretical derivation. This is, for example, the case of the one-dimensional quasi-linear theory for the electron-beam-plasma interaction problem [2].

For this reason we make an effort [3] to find an efficient general method to solve equations occurring in the weak turbulence theory. In the literature various types of interactions have already been treated successfully by numerical means. As early as in 1962 Drummond and Pines [4] treated the Langmuir-wave-particle interaction in a 1-D system numerically. In the last few years three-wave and wave-wave-particle interactions have been numerically studied as initial value problems in 1-D and 2-D systems e.g. in [5-8]. In all of these papers the wave-particle interaction has not

been treated consistently. In this paper we present a numerical approximation for the Langmuir wave-particle interaction in a 2-D plasma. Subsequently we apply the method to an open problem [9]: the evolution of electron-beam excited Langmuir turbulence in a multi-dimensional system.

2. QUASILINEAR THEORY

The velocity distribution of charged particles in a collisionless plasma may evolve due to interactions with waves in the plasma. There are basically two types of interactions: resonant and non-resonant. Particles interacting resonantly with waves have a velocity which equals the waves phase velocity whereas the non-resonant particles just act as the wave supporting medium. Kaufman [10] has given a very transparent formulation of the quasilinear theory, where the temporal evolution of the lowest order distribution function is determined by merely resonant interactions. The non-resonant term in his case is decoupled from the equation but is needed to ensure conservation of energy and momentum.

We give Kaufman's equations generalized to more dimensions ($\nu = D, \nu = 1, 2$ or 3) and normalized according to

$$\begin{aligned} k &\longrightarrow k/r_d, & v &\longrightarrow v v_{th}, & t &\longrightarrow t/\omega_p, \\ f &\longrightarrow f n / v_{th}^\nu, & \mathcal{E}_{\underline{k}} &\longrightarrow 4\pi n T r_d^\nu \mathcal{E}_{\underline{k}}. \end{aligned} \quad (1)$$

Here k denotes the wave number, r_d is the Debye radius, v_{th} the electron thermal velocity, ω_p the plasma frequency, n and T are the electron density and temperature, respectively, and $\mathcal{E}_{\underline{k}}$ is the spectral density of the electric field. The kinetic equation for the particle distribution reads then

$$\frac{\partial}{\partial t} f(\underline{v}, t) = \frac{\partial}{\partial \underline{v}} \cdot \underline{D} \cdot \frac{\partial}{\partial \underline{v}} f(\underline{v}, t), \quad (2)$$

An easy way to ensure similar treatment of both δ -functions is to evaluate both of them under a velocity-integral. Having this in mind, we use the weak form [11] of the diffusion equation, i.e. we multiply Eq.(2) by an arbitrary test function, $g(\underline{v})$, and integrate over a velocity space domain Ω :

$$\int_{\Omega} g(\underline{v}) \frac{\partial f(\underline{v}, t)}{\partial t} d^{\nu}v = \int_{\Omega} g(\underline{v}) \frac{\partial}{\partial \underline{v}} \cdot \underline{D} \cdot \frac{\partial}{\partial \underline{v}} f(\underline{v}, t) d^{\nu}v . \quad (8)$$

This is to hold for each $g(\underline{v})$ in some test space G and for each $t > 0$. By partial integration of the right hand side we obtain

$$\int_{\Omega} \left(g \frac{\partial f}{\partial t} + \frac{\partial g}{\partial \underline{v}} \cdot \underline{D} \cdot \frac{\partial f}{\partial \underline{v}} \right) d^{\nu}v = \oint_{\partial \Omega} g d^{\nu}\sigma \cdot \underline{D} \cdot \frac{\partial f}{\partial \underline{v}} , \quad \forall g(\underline{v}) \in G. \quad (9)$$

Here $d^{\nu}\sigma$ denotes the directed surface element of the ν -dimensional domain. Apart from some mathematical subtleties, Eq.(9) is equivalent to the original differential equation (2) [11]. The equation (9) is the starting point for the discretization. Conveniently the solution of the problem is sought in the space G . The most popular linear space to imbed this problem is the Sobolev space $H^1(\Omega)$.

4. NUMERICAL APPROXIMATION

4.1 Finite Velocity Domain

Let us use the Ritz-Galerkin method [11] for the discretization of the weak form, Eq.(9). The method searches for solutions of Eq.(9) for g and f lying in a finite dimensional subspace S^N of $H^1(\Omega)$. First we need to specify Ω . We might get rid of the boundary term in Eq.(9) by specifying Ω to be the whole velocity space ($|\underline{v}| \leq \infty$) together with the physically reasonable assumption that f and $\partial f / \partial \underline{v}$ vanish at infinity. However, having finite element subspaces of $H^1(\Omega)$ in mind, we need a finite domain

where the diffusion tensor is given by

$$\underline{D}(\underline{v}, t) = \pi \int \frac{d^3k}{(2\pi)^3} \frac{\underline{k} \underline{k}}{k^2} \epsilon_{\underline{k}} \delta(\omega - \underline{k} \cdot \underline{v}). \quad (3)$$

The waves evolve according to the "linear" law,

$$\partial \epsilon_{\underline{k}} / \partial t = 2 \gamma_{\underline{k}} \epsilon_{\underline{k}}, \quad (4)$$

with a slowly varying increment

$$\gamma_{\underline{k}} = \frac{\pi}{k^2} \frac{\partial \epsilon / \partial \omega}{\partial \epsilon / \partial \omega} \int \underline{k} \cdot \frac{\partial f}{\partial \underline{v}} \delta(\omega - \underline{k} \cdot \underline{v}) d^3v \quad (5)$$

Where

$$\partial \epsilon / \partial \omega = 2 + 3k^2 \quad (6)$$

and

$$\omega = 1 + 3/2 k^2. \quad (7)$$

3. THE WEAK FORM OF THE DIFFUSION EQUATION

The equations (2) and (4) show a certain similarity due to the fact that the only interaction considered is the wave-particle-interaction. The wave-particle operator is represented by $\delta(\omega - \underline{k} \cdot \underline{v})$ on the right hand sides of both equations. A consistent numerical approximation can be expected, if these δ -functions are treated in the same way in both equations. By consistent we mean that the system conserves well energy and momentum.

$$\Omega, \text{ i.e. } \Omega = \{ \underline{v} \mid v_{xe} \leq v_x \leq v_{xu}, v_{ye} \leq v_y \leq v_{yu} \}.$$

As a first approximation step we neglect the boundary term in Eq.(9). This can be interpreted in two different ways. We understand it either as the application of a natural boundary condition,

$$d\underline{v} \cdot \underline{D} \cdot \partial f / \partial \underline{v} = 0, \quad (10)$$

everywhere on $\delta\Omega$, or as the application of an essential boundary condition,

$$f(\underline{v}, t) = 0, \quad (11)$$

on $\delta\Omega$. Equation (11) is called an essential condition, since it has to be imposed on the functional space, whereas Eq.(10) is automatically satisfied by just neglecting the right hand side of Eq.(9). Comparative applications of Eqs.(10) and (11) will give us a measure for the error committed by using a finite Ω instead of the infinite velocity space.

For ease of reference we will use the notation $H^1(\Omega)$ and $H_E^1(\Omega)$, the subscript E standing for "essential boundary condition".

4.2 Discrete Velocities

The velocity space is discretized by the introduction of a finite dimensional subspace S^N of $H^1(\Omega)$

$$S^N = \text{span} \{ \psi_1^N, \psi_2^N, \psi_3^N, \dots, \psi_N^N \}. \quad (12)$$

The test function g and the approximate solution f_N of Eq.(9) are assumed to lie in S^N , i.e.

$$g(\underline{v}) = \psi_j^N, \quad j = 1, \dots, N, \quad (13)$$

$$f_N(\underline{v}, t) = \sum_{j=1}^N f_j(t) \psi_j^N(\underline{v}). \quad (14)$$

As in the case of $H_E^1(\Omega)$ we use the subscript E on S_E^N to indicate restriction by the essential boundary condition, Eq.(11). The discrete approximation of Eq.(9) reads then:

$$\sum_{j=1}^N \left\{ \frac{df_j}{dt} \int_{\Omega} \psi_i \psi_j d^N v + f_j \int_{\Omega} \frac{\partial \psi_i}{\partial v} \cdot \underline{D} \cdot \frac{\partial \psi_j}{\partial v} d^N v \right\} = 0, \quad (15)$$

$$i = 1, \dots, N.$$

Here we have made use of Eq.(10) if ψ_j is understood to belong to S^N , or we have made use of Eq.(11), if ψ_j belongs to S_E^N . Equation (15) is a system of N ordinary differential equations of first order for the expansion coefficients $f_j(t)$. The system may conveniently be written in matrix form

$$\underline{A} \cdot \partial \underline{f} / \partial t = \underline{B} \cdot \underline{f}, \quad (16)$$

where

$$A_{ij} = \int_{\Omega} \psi_i \psi_j d^N v, \quad (17)$$

$$B_{ij} = - \int_{\Omega} \frac{\partial \psi_i}{\partial v} \cdot \underline{D} \cdot \frac{\partial \psi_j}{\partial v} d^N v \quad (18)$$

and

$$\underline{f}(t) = (f_1, \dots, f_N). \quad (19)$$

Note that $\underline{\underline{A}}$ and $\underline{\underline{B}}$ are symmetric, since the diffusion tensor, Eq.(3), is symmetric. $\underline{\underline{A}}$ and $-\underline{\underline{B}}$ are positive definite. They can be made sparse, if spaces S^N of type "finite-element" are chosen.

We use piecewise linear, continuous basis functions ψ_i , i.e. roof functions in the 1-D case, and pyramids in the 2-D case, respectively. The 1-D velocity mesh is denoted by v_1, \dots, v_N . The supports of the pyramids are constructed according to Fig. 1. The rectangular (v_x, v_y) -mesh is non-equidistant. The 2-D basis function is given by the pyramid which takes the value 1 in point G and is zero on the whole contour ABCDEFA. We numerate the mesh-points according to Fig. 2.

4.3 Finite Wave Vector Domain

The wave vector domain, $\Xi = \{ \underline{k} \mid k_{x\ell} \leq k_x \leq k_{xu}, k_{y\ell} \leq k_y \leq k_{yu} \}$ is chosen such, that every important part of the spectrum, $\mathcal{E}_{\underline{k}}(t)$, lies within the domain during the whole evolution. Ξ should, on the other hand, be as small as possible to allow for high k-resolution. A good choice for Ξ can usually be made only after several tentative solutions of the whole problem.

4.4 Discrete Waves

The simplest way to discretize the waves is the classical one, i.e. one assumes that the system is closed to a ν -dimensional box of volume $V_\nu = L_1 \dots L_\nu$. The discrete k's are then given by

$$\underline{k} = \left(\frac{2\pi}{L_1} \delta_1, \dots, \frac{2\pi}{L_\nu} \delta_\nu \right), \quad \delta_j = 0, \pm 1, \pm 2, \dots \quad (20)$$

They are equidistant in each direction. Here \underline{k} and V_ν may be understood to be dimensionless ($V_\nu \rightarrow V_\nu r_d^\nu$). The diffusion tensor, Eq.(3), takes

then the form

$$\underline{D}(\underline{v}, t) = \pi \sum_{\underline{k}} \frac{\underline{k} \cdot \underline{k}}{k^2} I_{\underline{k}} \delta(\omega - \underline{k} \cdot \underline{v}), \quad (21)$$

with

$$I_{\underline{k}} = \varepsilon_{\underline{k}} / V_{\nu}, \quad (22)$$

$I_{\underline{k}}$ being essentially the wave energy per discrete mode (see paragraph 5.1). The equation (4) holds also for $I_{\underline{k}}$:

$$dI_{\underline{k}} / dt = 2 \gamma_{\underline{k}} I_{\underline{k}}. \quad (23)$$

This simple discretization works well in the 2-D case. In 1-D however, the approximation was essentially improved by taking non-equidistant k -values. The point is that equidistant k 's result in non-equidistant phase velocities,

$$\varphi_k = \omega / k = 1/k + 3/2 k. \quad (24)$$

For a reasonable numerical approximation of the wave-particle interaction it is necessary that a velocity cell is influenced by at least one wave. This means in the one-dimensional case, that there is for each interval (v_i, v_{i+1}) at least one φ_k such that $v_i < \varphi_k < v_{i+1}$.

With an equidistant k -mesh this can only be ensured by a high number of waves. Some v -intervals will then comprise e.g. 10 waves and others merely one, which is certainly a bad repartition of the numerical degrees of freedom and hence a bad approximation. Because of the one-to-one correspondence between one-dimensional k and v , it is desirable to fix the φ_k -values according to the v -mesh. One chooses conveniently one wave per velocity interval $[v_i, v_{i+1}]$

$$\varphi_i = (v_{i+1} + v_i) / 2. \quad (25)$$

Consistently with Eq.(7) one defines the frequency and the wave vector,

$$k_i = k(\varphi_i) \equiv (\varphi/3) \left[1 - (1 - 6/\varphi^2)^{1/2} \right]_{\varphi = \varphi_i} . \quad (26)$$

One also defines the length of a k-interval by

$$\lambda_i = k(v_{i+1}) - k(v_i), \quad (27)$$

using the definition for $k(v)$ given by Eq.(26). We may then approximate the diffusion coefficient, Eq.(3), by

$$D(v, t) = \pi \sum_i I_i(t) \delta(\omega - k_i v). \quad (28)$$

Thereby understanding that

$$I_i = \lambda_i \mathcal{E}_i / 2\pi. \quad (29)$$

It is possible to imagine more sophisticated ways to discretize the waves than those described. One could use e.g. a finite element approximation for the continuous \mathcal{E}_k ,

$$\mathcal{E}_k(t) = \sum_{i=1}^M e_i(t) \chi_i(k), \quad (30)$$

where $\chi_i(k)$ are piecewise constant functions.

If in 1-D the support of χ_i is chosen to be $(k_i, k_i + \lambda_i)$, this method is equivalent to the method used for Eq.(28), if the additional approximation

$$\int_{k(v_i)}^{k(v_i) + \lambda_i} 1/k dk \approx \lambda_i / k_i \quad (31)$$

is used.

Thus this ansatz brings nothing essentially new in the 1-D case. However, it can be shown that it improves but also complicates the method in the 2-D case. The increased programming effort might only be worthwhile for special applications.

4.5 Wave-Particle Interaction

One-dimensional case

Since the basis functions ψ_i are piecewise linear it is straightforward to give the explicit form of the matrix B_{ij} , Eq.(18)

$$B_{ij} = -2\pi \sum_{\kappa}^+ \frac{1}{k_{\kappa}} \psi_i'(\varphi_{\kappa}) \psi_j'(\varphi_{\kappa}) I_{\kappa} . \quad (32)$$

The prime ' stands for d/dv . The sum \sum^+ extends only over $k_{\kappa} > 0$; therefore a factor 2 has been inserted in front of the π . Only the elements $B_{i \ i-1} = B_{i-1 \ i}$ and B_{ii} are non-zero. One wave only out of the sum contributes to an element $B_{i \ i-1}$, whereas two waves contribute to B_{ii} , viz.

$$B_{i-1 \ i} = \frac{2\pi}{(v_i - v_{i-1})^2} \frac{1}{k_i} I_i , \quad (33)$$

$$B_{ii} = -\frac{2\pi}{(v_i - v_{i-1})^2} \frac{1}{k_{i-1}} I_{i-1} - \frac{2\pi}{(v_{i+1} - v_i)^2} \frac{1}{k_i} I_i .$$

It is equally easy to get the expression for the increment, Eq.(5),

$$y_i = \frac{f_{i+1} - f_i}{v_{i+1} - v_i} \left[\frac{\pi}{k^2 \partial \epsilon / \partial \omega} \right]_{k=k_i} . \quad (34)$$

Two-dimensional case

Here the matrix \underline{B} takes the form

$$B_{ij} = -2\pi \sum_{\underline{k}}^+ \frac{I_{\underline{k}}}{k} \int_{C_{\underline{k}}} ds \left(\frac{\partial \psi_i}{\partial \underline{v}} \cdot \hat{\underline{k}} \right) \left(\frac{\partial \psi_j}{\partial \underline{v}} \cdot \hat{\underline{k}} \right). \quad (35)$$

The sum \sum^+ is restricted on $k_x > 0$. The quantity ds is a line element in the velocity space and the straight line $C_{\underline{k}}$ is defined by

$$C_{\underline{k}} = \{ \underline{v} / \underline{k} \cdot \underline{v} - \omega = 0 \}. \quad (36)$$

Commonly we call $C_{\underline{k}}$ the interaction line of the wave \underline{k} because all particles which interact with the wave \underline{k} lie on $C_{\underline{k}}$. Since the integral is piecewise constant, we may write Eq.(35) as

$$B_{ij} = -2\pi \sum_{\underline{k}}^+ \frac{I_{\underline{k}}}{k} \sum_{\Delta \cap C_{\underline{k}} \neq \emptyset} s_{\Delta}(\underline{k}) \left(\frac{\partial \psi_i}{\partial \underline{v}} \cdot \hat{\underline{k}} \right) \left(\frac{\partial \psi_j}{\partial \underline{v}} \cdot \hat{\underline{k}} \right), \quad (37)$$

where the second sum extends over all triangles Δ which are cut by the interaction line $C_{\underline{k}}$. The quantity $s_{\Delta}(\underline{k})$ denotes the length of $C_{\underline{k}}$ within the triangle Δ , and $\hat{\underline{k}}$ is the unit vector in \underline{k} -direction.

Practically the matrix $\underline{\underline{B}}$ is constructed in the following way. We separate time dependent and time independent parts

$$B_{ij}(t) = \sum_{\underline{k}}^+ B_{ijk} I_{\underline{k}}(t), \quad (38)$$

where the definition of the constant matrices B_{ijk} is clear from comparison with Eq.(37). They can be calculated once forever together with matrix $\underline{\underline{A}}$, Eq.(17).

The band-width of the matrices $\underline{\underline{A}}$ and $\underline{\underline{B}}$ is $2n_y + 3$. If their symmetry is used, $n_y + 2$ elements per row have to be calculated.

A formula rather similar to Eq.(38) can be obtained for the increment γ ,

Eq.(5),

$$\underline{\gamma}_k(t) = \sum_i \Gamma_{ki} f_i(t) \quad (39)$$

Here

$$\Gamma_{ki} = \frac{\pi}{k^2 \partial \epsilon / \partial \omega} \sum_{\Delta n C_k \neq 0} S_{\Delta}(k) \hat{k} \cdot \frac{\partial \psi_i}{\partial \underline{u}} \quad (40)$$

4.6 Discrete Time

The system of ordinary differential equations to be solved in time is given by Eqs.(16) and (23):

$$\begin{aligned} \underline{A} \cdot \partial \underline{f} / \partial t &= \underline{B}(t) \cdot \underline{f} , \\ d\underline{I}_k / dt &= 2 \underline{\gamma}_k(t) \underline{I}_k . \end{aligned} \quad (41)$$

One notes that the time dependence of $\underline{B}(t)$ is given by $\underline{I}_k(t)$, (Eq.(38)), and the time dependence of $\underline{\gamma}_k(t)$ is given by $\underline{f}(t)$, (Eq.(39)). This particular form of the system, (Eq.(41)), suggests a four level scheme for the discretization in time. In fact a fully time centered scheme can be obtained on an equidistant time mesh. Let t_1, t_2, t_3, t_4 be four equally spaced consecutive times. The discrete approximation of Eq.(41) then looks like

$$\begin{aligned} \underline{A} \cdot [\underline{f}(t_3) - \underline{f}(t_1)] / (t_3 - t_1) &= \underline{B}(t_2) \cdot [\underline{f}(t_1) + \underline{f}(t_3)] / 2 , \\ [\underline{I}_k(t_4) - \underline{I}_k(t_2)] / (t_4 - t_2) &= \underline{\gamma}_k(t_3) [\underline{I}_k(t_2) + \underline{I}_k(t_4)] . \end{aligned} \quad (42)$$

Knowing \underline{f} at time t_1 and \underline{I}_k at time t_2 one can solve the first equation for \underline{f} at time t_3 by a Gauss elimination. Then \underline{I}_k at t_4 can be obtained from the second equation.

Equation (41) describes a diffusion-like process. In such a process the time derivatives decrease in the course of time. The time step should therefore be adjusted. We used an automatic time step control allowing the step to change not more than 10%, i.e. $|(t_4 - t_3)/(t_2 - t_1) - 1| < 1/10$. Due to this constraint the time centering of Eq.(42) stays almost undamaged.

5. DIAGNOSTICS

5.1 The Conserved Quantities

Let us define in dimensionless form the total particle density,

$$\mathcal{N} = \int f(\underline{v}, t) d^{\nu}v, \quad (43)$$

the particle momentum density,

$$\underline{P}_p = \int \underline{v} f(\underline{v}, t) d^{\nu}v, \quad (44)$$

the wave momentum density,

$$\underline{P}_w = \frac{1}{2} \int \frac{d^{\nu}k}{(2\pi)^{\nu}} \underline{E}_k k \frac{\partial \epsilon}{\partial \omega}, \quad (45)$$

the particle energy density,

$$W_p = \frac{1}{2} \int v^2 f d^{\nu}v, \quad (46)$$

and the wave energy density,

$$W_w = \frac{1}{2} \int \frac{d^{\nu}k}{(2\pi)^{\nu}} \underline{E}_k \omega \frac{\partial \epsilon}{\partial \omega}. \quad (47)$$

From the diffusion equation, Eq.(2), it is easy to derive the conservation of the total particle density

$$dN/dt = 0, \quad (48)$$

and it has been shown by Kaufman [10] that the total momentum density,

$$\underline{P} = \underline{P}_p(t) + \underline{P}_w(t) \quad (49)$$

and the total energy density

$$W = W_p(t) + W_w(t) \quad (50)$$

are conserved.

The energy conservation law may serve as a diagnostic of our numerical method, the total energy being sensitive to errors in both the distribution function and the spectral density. For natural boundary condition, Eq.(10) the total particle density is exactly conserved by our method as can be seen by noting that

$$1 = \sum_i \psi_i \quad (51)$$

and

$$dN/dt = \int 1 \dot{f} d^3v = \sum_{ij} A_{ij} \dot{f}_j \quad (52)$$

Use of Eqs.(16) and (18) leads then to

$$dN/dt = \sum_j f_j \int \left(\frac{\partial}{\partial \underline{u}} \sum_i \psi_i \right) \cdot \underline{D} \cdot \frac{\partial \psi_i}{\partial \underline{u}} d^3v = 0. \quad (53)$$

With a similar argument it can be shown that from the exact relation

$$\underline{v} = \sum_i (\underline{v})_i \psi_i \quad (54)$$

it follows that \underline{P}_p is exactly treated by our numerical method.

5.2 H-Theorem

Let us define

$$H = \frac{1}{2} \int f^2 d^{\nu}v \quad (55)$$

with the use of Eq.(2) one can show that |12|

$$dH/dt = - \int \frac{\partial f}{\partial \underline{v}} \cdot \underline{D} \cdot \frac{\partial f}{\partial \underline{v}} d^{\nu}v \leq 0. \quad (56)$$

This monotony is preserved by the numerical method,

$$dH/dt = \underline{f} \cdot \underline{A} \cdot \dot{\underline{f}} = \underline{f} \cdot \underline{B} \cdot \underline{f} \leq 0, \quad (57)$$

as can be seen from Eqs.(14), (16), (17), and (18).

5.3 Spectral Moments

In order to describe the evolution of the spectrum, we introduce a few moments. Using the wave energy density per k-interval,

$$W_{\underline{k}} = \frac{1}{2} \sum_{\underline{k}} \omega \partial \epsilon / \partial \omega, \quad (58)$$

we define the location of the spectrum in k-space,

$$\langle \underline{k} \rangle \equiv \int \frac{d^{\nu}k}{(2\pi)^{\nu}} \underline{k} W_{\underline{k}} / W_N, \quad (59)$$

and the mean width of the spectrum

$$\Delta k_a \equiv \left[\int \frac{d^{\nu} k}{(2\pi)^{\nu}} (k_a - \langle k_a \rangle)^2 W_{\underline{k}} / W_w \right]^{1/2}, \quad a = x, y. \quad (60)$$

6. APPLICATION TO ELECTRON BEAM EXCITED LANGMUIR TURBULENCE

6.1 Physical Initial Conditions

We model the initial beam-plasma-system by two Maxwellian functions,

$$f(\underline{v}, t=0) = \frac{1}{(2\pi)^{\nu/2} (1+\xi)} \left\{ \exp(-\frac{1}{2} \underline{v}^2) + \xi \exp(-\frac{1}{2} (\underline{v}-\underline{u})^2) \right\}. \quad (61)$$

The ratio of the beam density to the plasma density is denoted by ξ . The beam has a velocity \underline{u} . Equal thermal spread of the plasma and the beam are assumed.

6.2 One-Dimensional Case

The evolution of electron beam excited Langmuir turbulence in a strongly magnetized plasma may be modelled by the 1-D quasilinear equations. A numerical solution to these equations has been given one and a half decades ago [4]. If we solve the same equations here, we do it as an apprentice's work.

We have solved the case of a high velocity beam ($u = 15$) with very small density. It has very small density ($\xi = 10^{-5}$) to ensure the applicability

of the quasilinear theory. Fig. 3 shows the particle distribution and the spectral function for five subsequent times $t_0 - t_4$. In this calculation we used 90 equidistant mesh-points. The "shock"-phenomenon, anticipated by Ivanov and Rudakov [13], is nicely seen. The energy is conserved up to less than 10^{-4} of the wave energy. The steepness of the "shock-front", which one might suspect to be dependent on the discretization, does not change if 180 mesh-points are used.

As a result one can say that the one-dimensional case does not pose any problem. Storage space and available computation time on a small machine such as ours (CDC Cyber) are largely sufficient to treat 1-D cases to any reasonable accuracy. This heavenly situation is unfortunately not preserved in 2-D calculations, whose features have therefore to be studied in detail.

6.3 Two-Dimensional Case

Most of the physical results of our 2-D calculations have already been published [14]. In this paper the numerical aspects of our work and the influence of spontaneous emission will be discussed.

Boundary condition

The introduction of a finite velocity space (see paragraph 4.1) does not create any trouble in 1-D but does in 2-D. In 1-D the velocity domain has simply to be chosen such that, at the boundary, no wave ever grows ($I(v_b) \approx 0$). From Eq.(28) follows then that $D(v_b) \approx 0$ and hence from Eq.(2) $f(v_b) \approx \text{const}$. In 2-D the wave-interaction lines always cut the boundary somewhere. And as long as not all wave-intensities are zero, diffusion takes place at the boundary. In Fig. 4, we show the influence of the boundary on the time evolution by using the natural boundary condition, Eq.(10), and the essential boundary condition, Eq.(11). Apart from the restriction, Eq.(11), the finite element spaces S^N and S_E^N are equivalent. We show the total wave energy W_w , Eq.(46), as a function of

time. The number of points was $N = 304$, and the number of waves $M = 285$. The velocity domain Ω was given by

$$\Omega = (\underline{v} | 3.8 \leq v_x \leq 10.8, -4.5 \leq v_y \leq 4.5)$$

and the wave vector domain by

$$\Xi = (\underline{k} | 0.1 \leq k_x \leq 0.215, -0.09 \leq k_y \leq 0.09).$$

The physical initial conditions were $\underline{u} = (9,0)$ and $\xi = 10^{-5}$. One observes no appreciable influence of the boundary up to the saturation time t_{sat} . During the 2-D diffusion phase ($t > t_{\text{sat}}$), however, the influence is remarkable. This coincides with the observation made on the particle distribution function across the beam, which is shown for t_{sat} and a final time t_F . For $t = t_F$ there is a 10% difference of the distribution function obtained from S^N and from S_E^N . The value of the wave energy at $t = t_F$ differs by 26% of $W_w(t_{\text{sat}})$. It can be concluded that qualitatively the physical phenomenon does not change due to the influence of the boundary. Accurate values for W_w , however, would need an extended velocity space and hence more points.

Initial fluctuations

Initially we assign to all wave intensities, Eq.(22), the same value I_0 . I_0 is determined by the input parameter

$$\eta = W_w(0) / [W_p(0) (k_{xu} - k_{xe})(k_{yu} - k_{ye})], \quad (62)$$

which is the ratio of the initial wave energy to the initial particle energy normalized to a k-domain of area 1. For an equilibrium plasma η is just the plasma parameter. In a beam-plasma system however, η depends not only on the density and temperature of the plasma but also on the history as how the beam has been introduced into the plasma. Moreover a more complete theory, including spontaneous emission, would have to be used. η stays therefore a free parameter.

We use I_0 not only as the initial value for $I_{\underline{k}}(t = 0)$ but also as a lower bound $I_{\underline{k}}(t) \gg I_0$. This brings something as "spontaneous emission" into our model. In a real system a wave will never completely damp out but will stay on some finite level due to spontaneous emission. To avoid the introduction of another free parameter we took I_0 for this finite level. Imposing the lower bound I_0 on $I_{\underline{k}}$ is equivalent to replacing Eq.(23) by

$$dI_{\underline{k}}/dt = 2\gamma_{\underline{k}}(I_{\underline{k}} - I_0) \quad (63)$$

for damped waves having an amplitude near I_0 . This means that energy is pumped to the mode \underline{k} at a rate $2|\gamma_{\underline{k}}|I_0 \omega \partial\epsilon/\partial\omega$ to prevent it to be damped below I_0 .

We are now able to discuss the useful range of η . In thermal equilibrium η may range from 10^{-10} in an interplanetary plasma up to 10^{-3} in a low temperature high density laboratory plasma. For the applicability of our model we have, however, to ensure that the "spontaneous emission", Eq.(63), does not directly influence the evolution of the particle distribution function although the energy conservation might be strongly influenced. A rough estimate for this criterion can be made by saying that the diffusion coefficient, Eq.(21), made up by waves of intensity I_0 should not influence the function f having a characteristic gradient length of Δv during the observation time t_{obs} :

$$(\Delta v)^2 / t_{obs} \gg D \approx \eta W_p(0) \pi (k_{yu} - k_{ye}) / |v| . \quad (64)$$

In Fig. 5 the influence of η on the wave energy evolution is shown. The saturation level does not depend on η for values lower than about $3 \cdot 10^{-7}$. The behaviour during the diffusion phase ($t \gg 2 \cdot 10^5$) seems also to be quite insensitive on η for $\eta \lesssim 3 \cdot 10^{-7}$. The criterion, Eq.(64), with $W_p(0) \approx 1$, $\Delta v_y \approx 2.5$ and $v \approx 6$ in the diffusion phase yields

$$\eta \ll 60 / t_{obs} . \quad (65)$$

At $t = 10^{-7}$ the result for $\eta = 3 \cdot 10^{-6}$ should still not be influenced very much by "spontaneous emission" during the calculation. The result, however, depends remarkably on the initial conditions.

We can conclude that there is no unique physical solution to the two-dimensional quasilinear equation for a beam-plasma system. The solution depends on the initial fluctuation level. The general features of the solution, however, do not depend on the initial conditions.

Conservation properties

In all runs we checked the deviations δN , δP and δW of the conserved quantities N , P and W , Eqs.(43), (49), and (50), from their initial values. As discussed in Eq.(53) δN must be given by the machine truncation errors. In fact on our machine $\delta N/N \sim 10^{-16}$. The relative error in the two momentum components was always smaller than $\delta W/W$. Therefore we show merely the evolution of the energy non-conservation δW in Fig. 6. It can be seen that the error δW decreases linearly with decreasing mesh-sizes in v and k .

Convergence properties

Extensive convergence studies are costly and unnecessary. Enough confidence into the method can be won by merely comparing the results of two runs with rather different mesh sizes. We have evaluated the spectral moments W_w , $\langle k_x \rangle$, Δk_x and Δk_y , Eqs.(47), (59), and (60) respectively, for the 2 runs describes in Fig. 6. The relative differences,

$$r(m) = \left(m_{300}(t) - m_{600}(t) \right) / m_{600}(t), \quad (66)$$

have been plotted versus time in Fig. 7. In Eq.(66) m stands for any of the quantities W_w , $\langle k_x \rangle$, Δk_x or Δk_y . The indices 300 and 600 refer to the two cases $N = M = 300$ and $N = M = 600$, respectively. It can be seen that the difference is 4 times smaller for the zero and the first order spectral moment, W_x and $\langle k_x \rangle$, than for the second order moments Δk_x and Δk_y , a result which is easily acceptable.

Mesh orientation

Since in our code we did not make use of the symmetry across the x-axis (Fig. 1) it was possible to turn the beam with respect to the mesh. In table 1 the saturation values W_{sat} for 3 different angles α between \underline{u} and the x-axis are shown. The case $N = M = 300$, $u = 9$, $\xi = 10^{-5}$, $\eta = 3 \cdot 10^{-6}$ is demonstrated. From the small deviation of 3% we got further confidence into the method.

7. CONCLUSION

We have presented a finite element method for the solution of two-dimensional quasilinear equations. Conservation and convergence properties are excellent. A draw-back of the method is the fact that it uses a finite velocity space which has to be larger the longer the calculation time is. With non-equidistant meshes, however, the errors introduced by the boundary can always be controlled.

The application of the method to the 2-D beam-plasma-problem has yielded the very important result that the solution depends sensitively on the initial fluctuations in contrast to the 1-D case.

The results suggest that our method might successfully be applicable to more complicated problems in weak turbulence theory. An ion-acoustic code is in progress.

ACKNOWLEDGMENT

We are indebted to Dr. R. Gruber for helpful discussions.

This work was supported by the Swiss National Science Foundation.

FIGURE CAPTIONS

- Figure 1: The support of a 2-D basis function.
- Figure 2: Example of a velocity mesh with $N = 20$ mesh-points.
- Figure 3: One-dimensional quasilinear evolution of a beam-plasma system.
- Figure 4: Influence of the finite velocity boundary on the evolution of the wave energy density $W_w(t)$ and the distribution $f(v_x = 6.6, v_y, t)$ across the beam. The finite element spaces $S_E^N(\text{---})$ and $S_E^N(\text{---})$ have been used.
- Figure 5: Influence of the initial fluctuations on the evolution of the wave energy density $W_w(t)$. The case $u_x = 9, \xi = 10^{-5}$ is shown.
- Figure 6: The numerical error δW in the energy conservation versus time. The case $u_x = 9, \xi = 10^{-5}, \eta = 3 \cdot 10^{-8}$ is shown. Two different meshes have been used: --- ($N = M = 300$) and --- ($N = M = 600$).
- Figure 7: Temporal evolution of the relative differences in the spectral moments between the $N = M = 300$ and the $N = M = 600$ case.
- Table 1 : Wave energy saturation value W_{sat} for three different angles α between the k_x -axis and the beam.

α	W_{sat}
$- 13^\circ$	6.89
0	6.70
$+ 13^\circ$	6.68

Table 1

REFERENCES

- |1| A.A. Vedenov, E.P. Velikhov, R.Z. Sagdeev, Nucl.Fusion 1 (1961) 82
- |2| R.C. Davidson, "Methods in Nonlinear Plasma Theory", Academic Press, New York 1972, ch. 9
- |3| K. Appert, Z.Angew.Math.Phys. 26 (1975) 663
- |4| W.E. Drummond, D. Pines, Nucl.Fusion, Suppl. 3 (1962) 1049
- |5| W.L. Kruer, E.J. Valeo, Phys.Fluids 16 (1973) 675
- |6| V.G. Makhankov, B.G. Shchinov, Comp.Phys.Comm. 4 (1972) 327
- |7| J.A. Fejer, Y.Y. Kuo, Phys.Fluids 16 (1973) 1490
- |8| N. Zabusky, J.H. Doles, F.W. Perkins, J.Geophys.Res. 78 (1973) 711
- |9| A.A. Ivanov, T.K. Sobolyeva, P.A. Yushmanov, Zh.Eksp.Teor.Fiz. 69 (1975) 2023
- |10| A.N. Kaufman, J.Plasma Phys. 8 (1972) 1
- |11| G. Strang, G.J. Fix, "An Analysis of the Finite Element Method", Prentice-Hall, Englewood Cliffs, 1973
- |12| I.B. Bernstein, F. Engelmann, Phys.Fluids 9 (1966) 937
- |13| A.A. Ivanov, L.I. Rudakov, Sov.Phys.JETP 24 (1967) 1027
- |14| K. Appert, T.M. Tran, J. Vaclavik, to be published

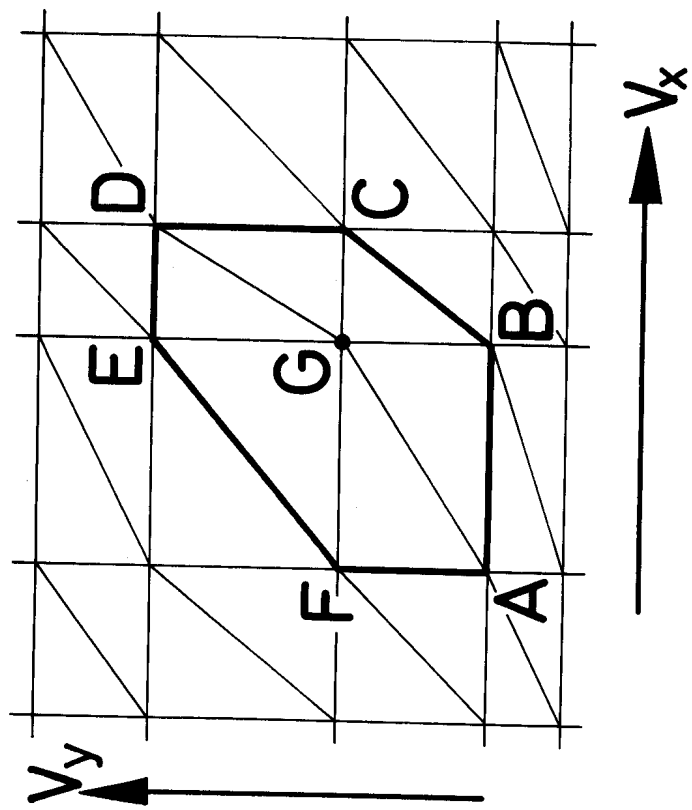


Fig.1

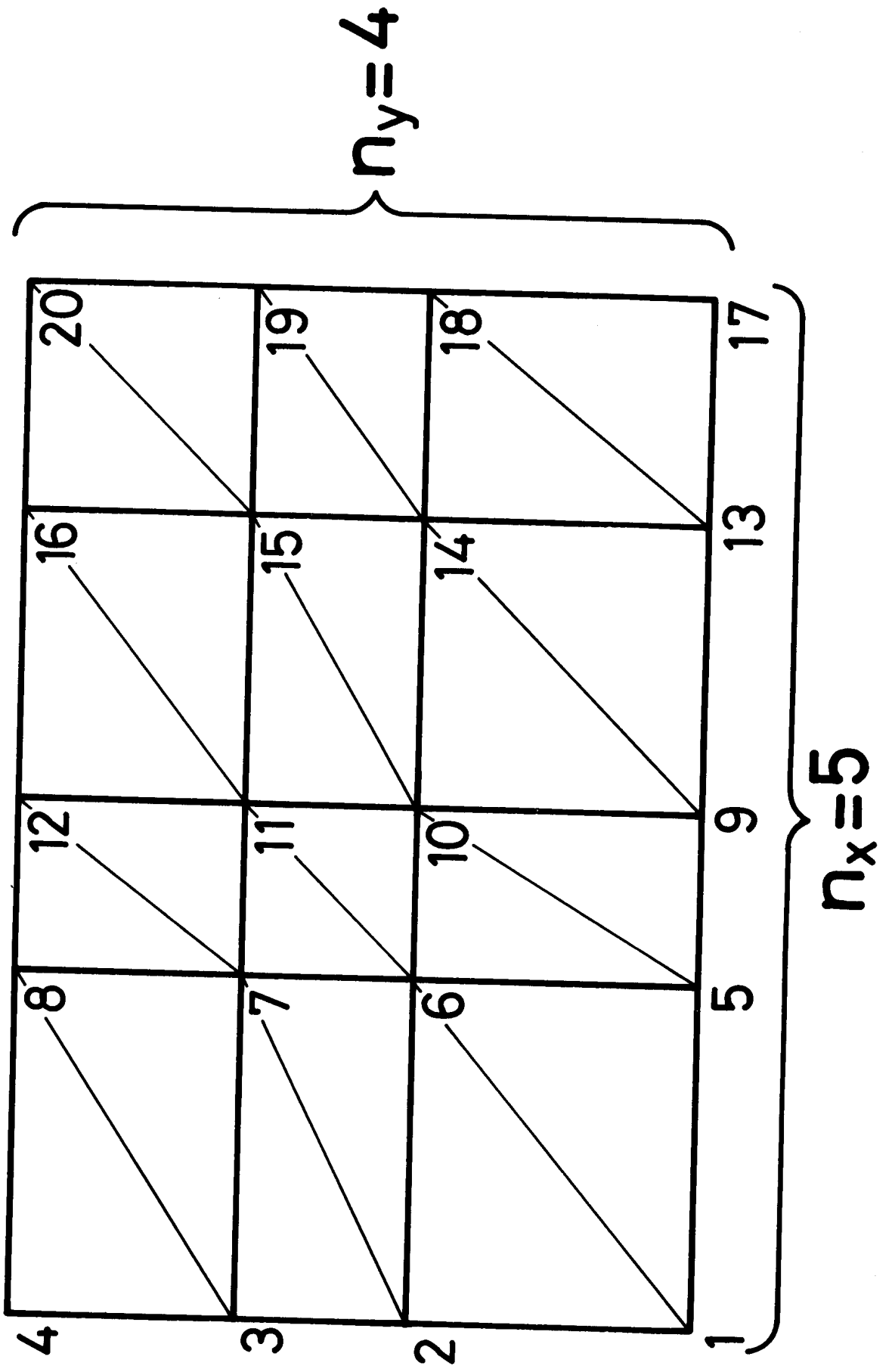


Fig. 2

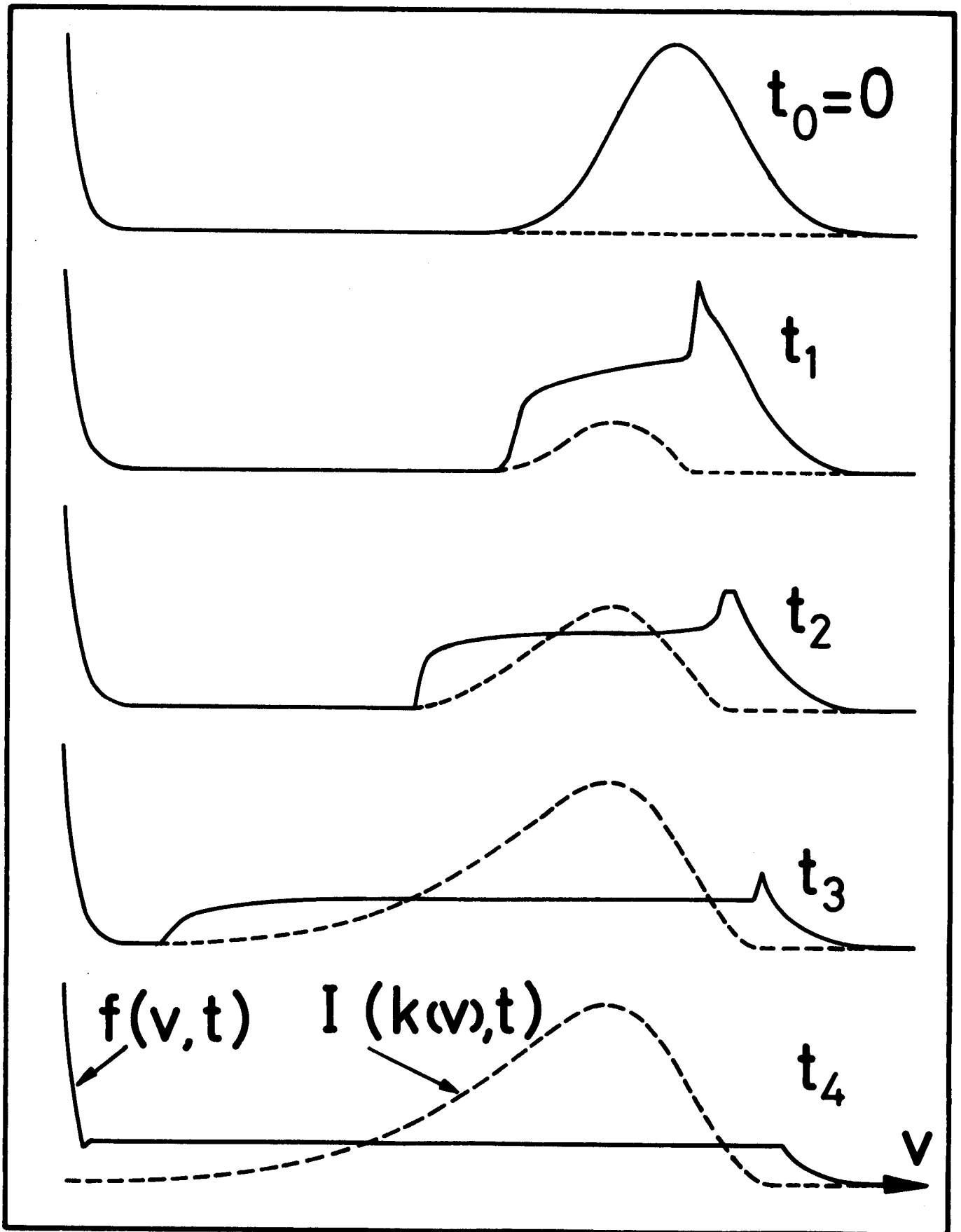


Fig. 3

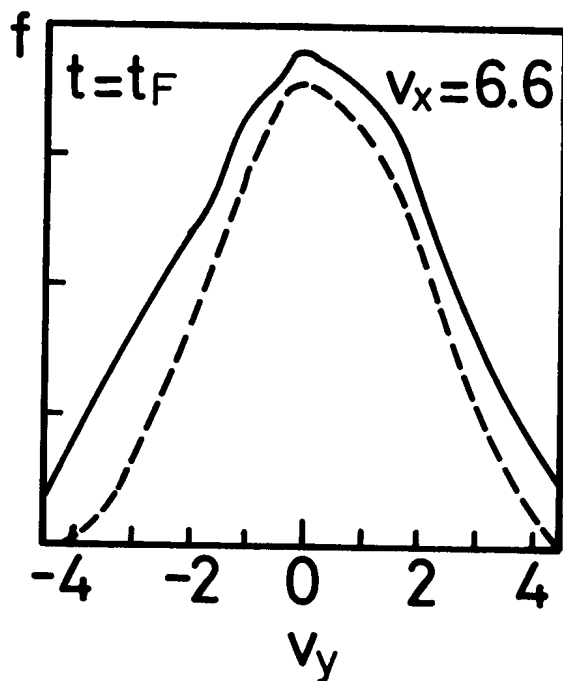
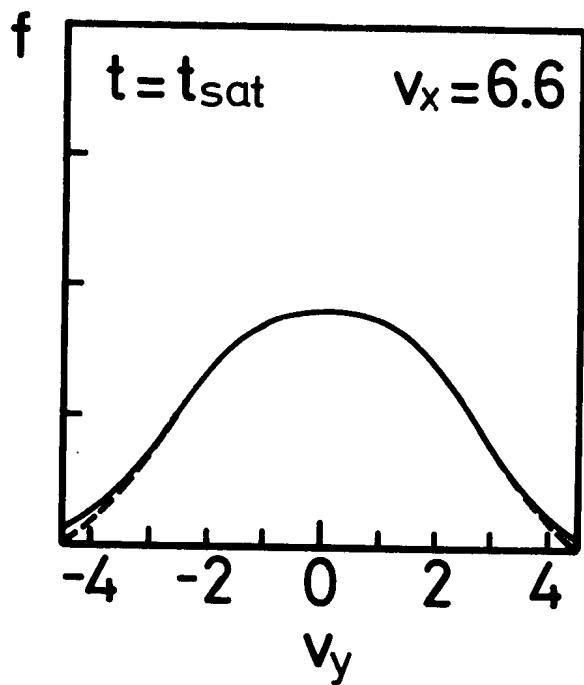
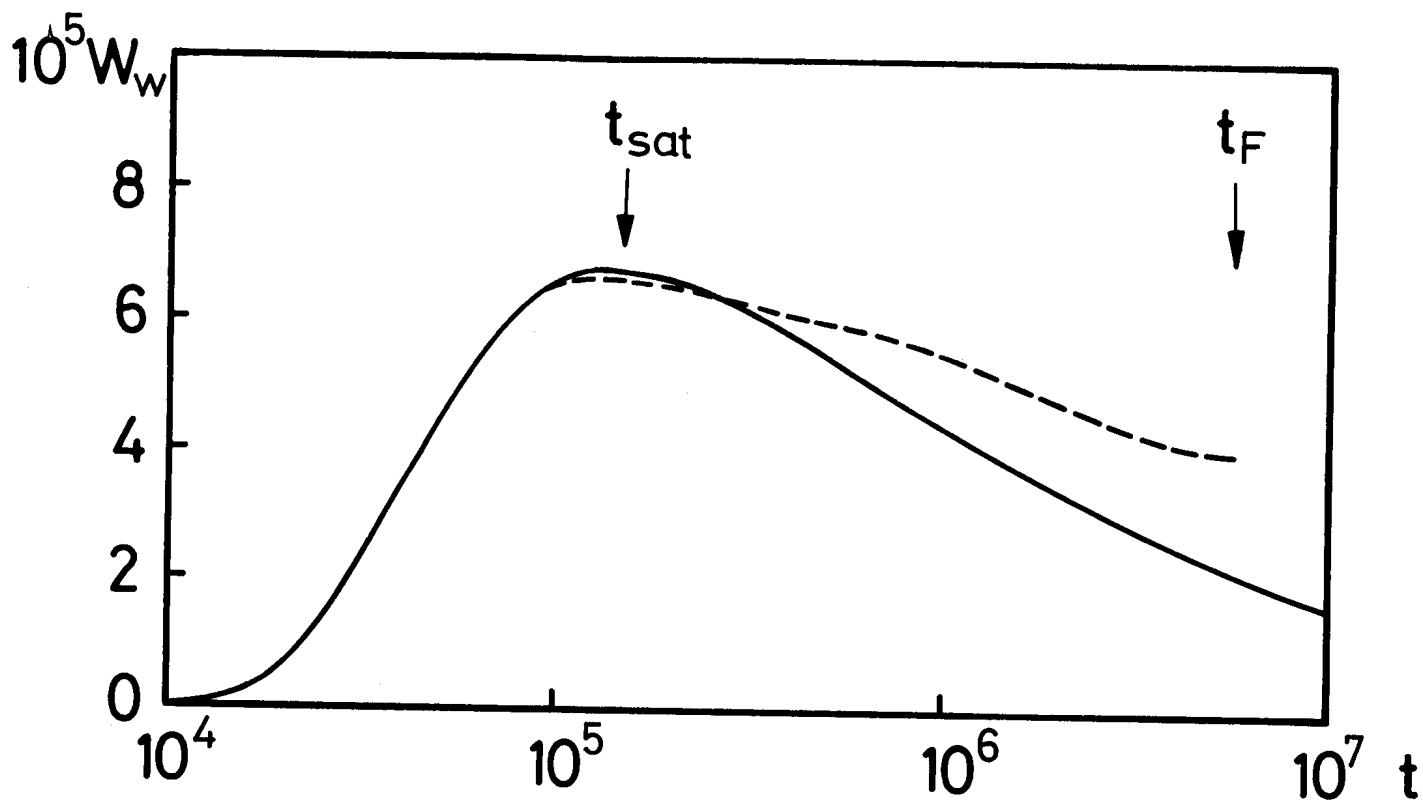


Fig. 4

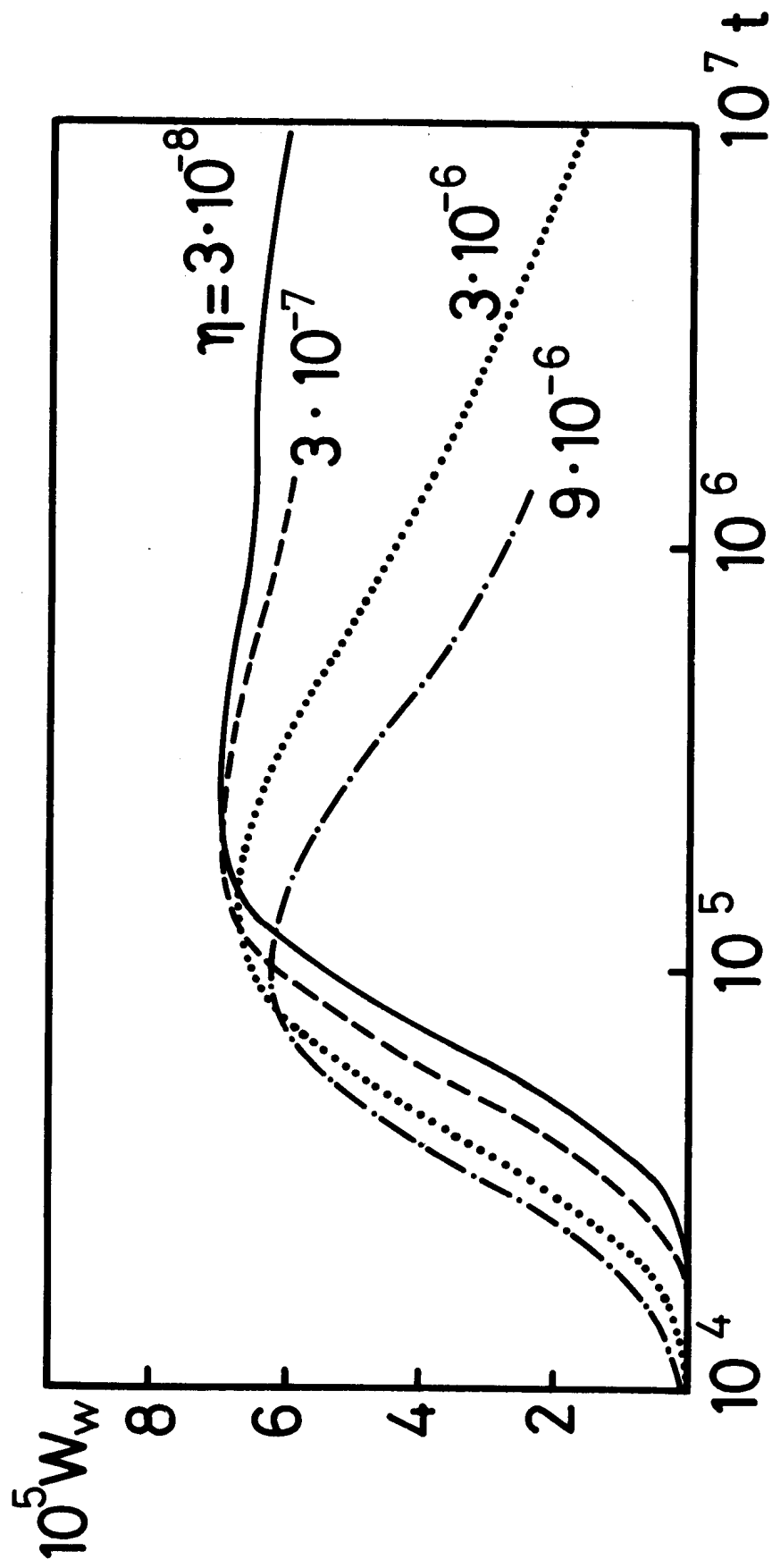


Fig.5

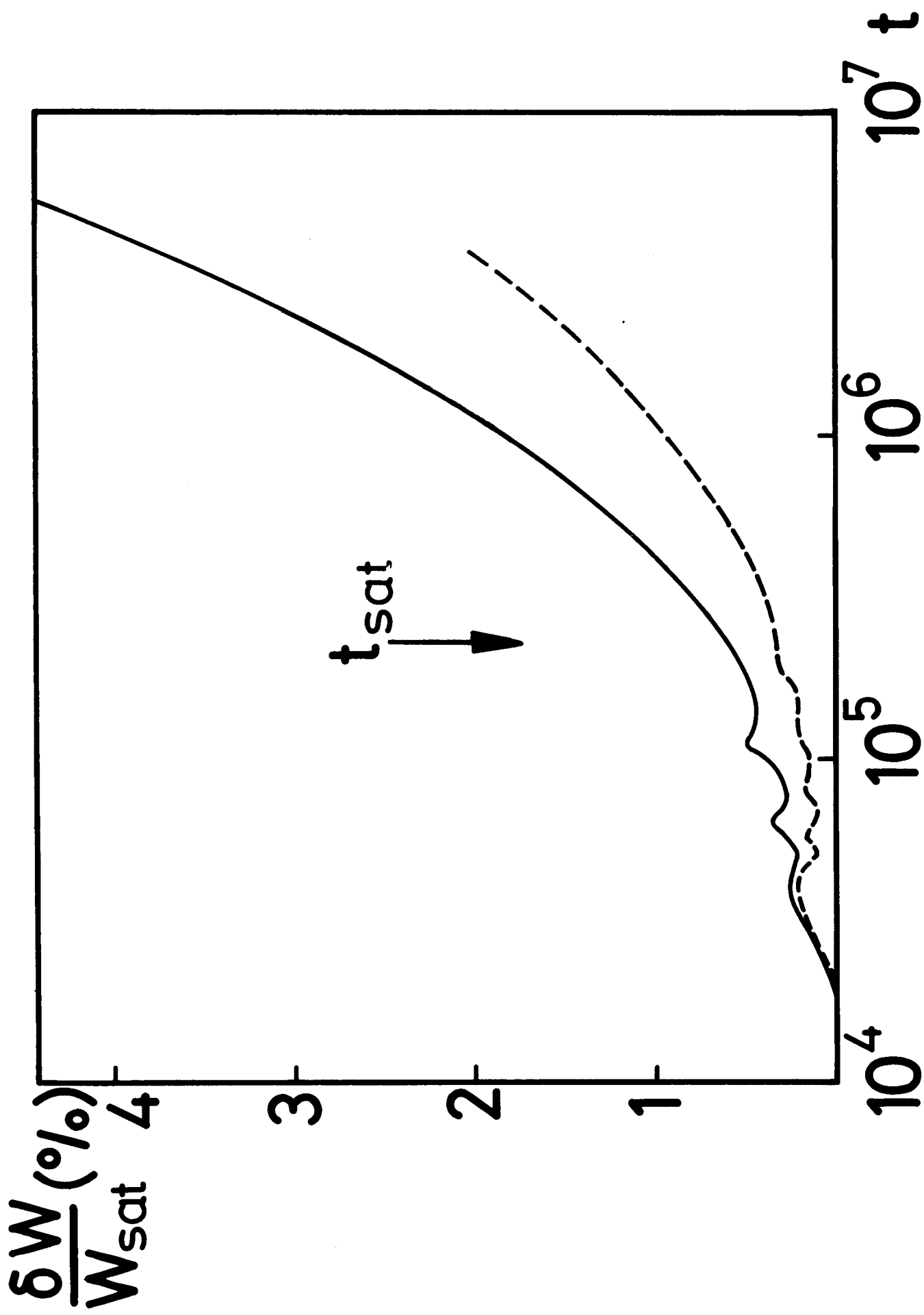


Fig.6

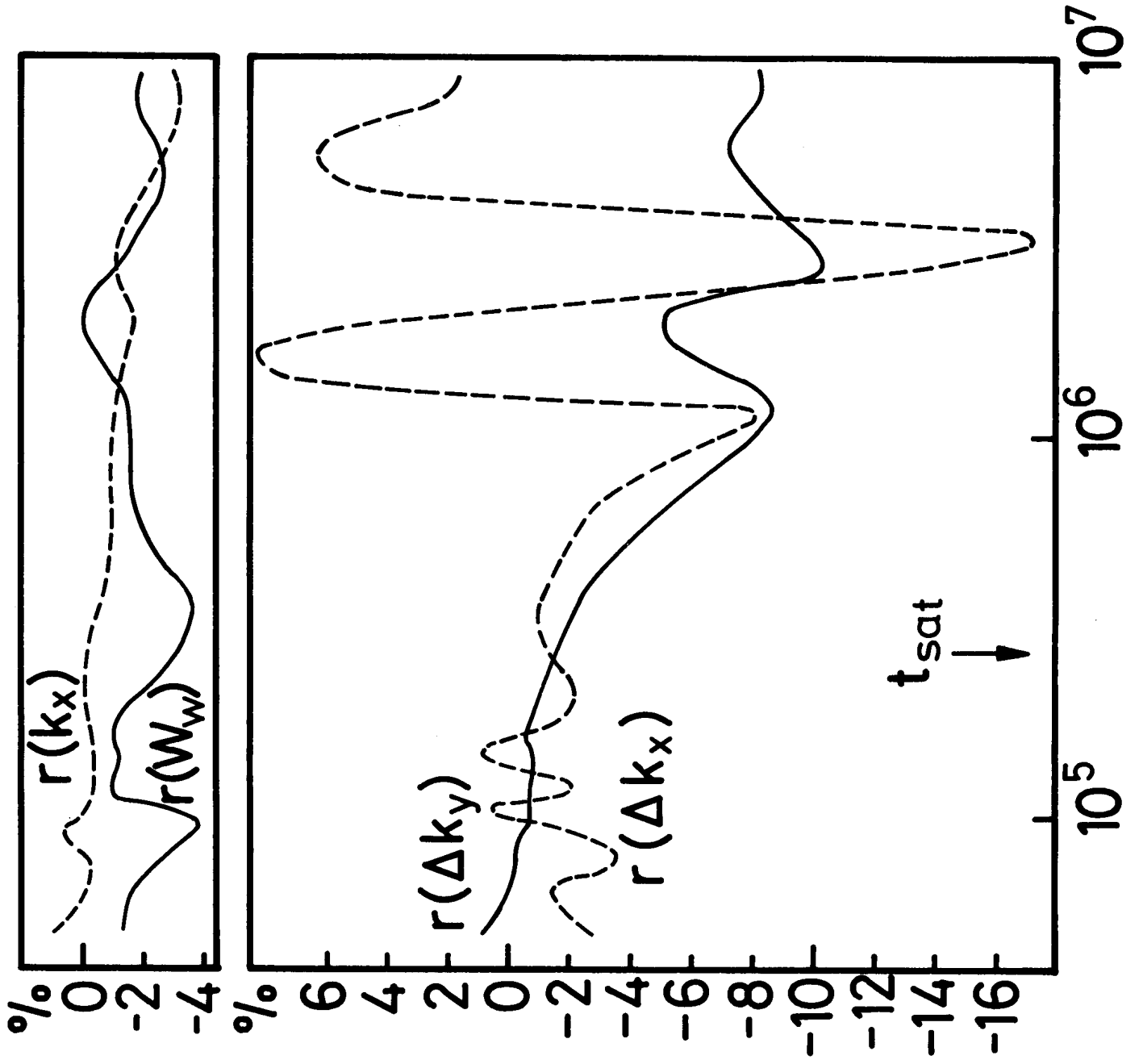


Fig.7